Applied Science, Computing and Energy, 2026, 4(5), 722-739

Groundwater Potential Mapping in Crystalline Basement Terrain Using an Integrated Geophysical–GIS Approach: Mubi, Northeastern Nigeria

David John Zirra and Umar Ibrahim Ashaka

Received: 17 March 2026/Accepted: 19 July 2026/Published: 28 July 2026

Abstract : *Groundwater is the primary source of water supply for domestic and agricultural purposes in Mubi and environs, northeastern Nigeria. This study integrates geological field mapping, vertical electrical sounding (VES), and hydrogeophysical parameter estimation to delineate groundwater potential zones within an area of approximately 216 km² (longitudes 13°12'00" E – 13°20'00" E; latitudes 10°12'00" N – 10°20'00" N). Detailed geological mapping reveals that the study area is underlain predominantly by porphyritic granite and fine-grained granite, with eluvial deposits occurring in the southwestern and southeastern portions. A total of 40 VES stations were surveyed using the Schlumberger electrode configuration, and data were interpreted using INTERPEX resistivity software. Quantitative interpretation identified four curve types: H (62%), KH (15%), A (10%), and QH (13%), indicating weathered and fractured/weathered aquifer systems. Aquifer characterization using Dar Zarrouk parameters shows that transverse resistance ranges from 12.38 $\Omega\cdot m^2$ to 5029.51 $\Omega\cdot m^2$ (mean: 1347.03 $\Omega\cdot m^2$), while longitudinal conductance ranges from 0.01 Ω^{-1} to 4.51 Ω^{-1} (mean: 0.69 Ω^{-1}). Based on longitudinal conductance, the aquifer protective capacity is classified as poor (5% of VES points), weak (12.5%), moderate (47.5%), and good (35%). Transmissivity values range from 5.89 $m^2\cdot d^{-1}$ to 748.78 $m^2\cdot d^{-1}$ (mean: 333.01 $m^2\cdot d^{-1}$). Aquifer potential rating based on transmissivity indicates moderate potential in 77.5% of the area, high potential in 17.5%, and low potential in 5%. Integration of these results with a GIS-based analytical hierarchy process using seven thematic layers (geology, land use/land cover, soil, rainfall, lineament density, drainage density, and slope) produced a groundwater potential map classifying the area into poor, moderate, and good potential zones. The consistency ratio of 0.0049 confirms the reliability of the analytical hierarchy process weighting. This study demonstrates that combining conventional geoelectrical methods with GIS-based multi-criteria decision analysis provides a robust framework for groundwater resource evaluation in crystalline basement terrains.*

Keywords: *Porphyritic granite; Vertical electrical sounding; Dar Zarrouk parameters; Aquifer transmissivity; Groundwater potential; Mubi; Nigeria*

David John Zirra*
Department of Geology, Federal University Dutsin-Ma, PMB 5000 Along Katsina-Kankara Road, Dutsin-Ma, Katsina State, Nigeria.
Email: djzira@fudutsinma.edu.ng
https://orcid.org/0009-0000-2616-7165

Umar Ibrahim Ashaka
Department of Geology, Federal University Dutsinma, PMB 5000 Along Katsina-Kankara Road, Dutsin-Ma, Katsina State, Nigeria.
Email: aumari@fudutsinma.edu.ng
https://orcid.org/0009-0001-7046-2417

1.0 Introduction

Water is a fundamental natural resource essential for sustaining human health, food security, ecosystem integrity, industrial development, and socio-economic growth. Freshwater availability is increasingly threatened by rapid population growth, urbanization, climate change, and unsustainable water resource exploitation.(National Water Policy, 1987).

The increasing global demand for freshwater, driven by population growth, urbanization, and climate variability, has placed unprecedented pressure on groundwater resources, particularly in arid and semi-arid regions of Africa and Asia (Manap *et al*., 2011; Das *et al*., 2017; Taylor *et al*., 2013). Groundwater supplies nearly half of the world's drinking water and approximately 43% of irrigation water, making it one of the most important freshwater resources for sustainable development.(Taylor *et al*., 2013).

In crystalline basement terrains, which underlie much of sub-Saharan Africa, groundwater occurrence is controlled by secondary porosity developed through weathering and fracturing of impermeable bedrock (Offodile, 1983; Foster and Chilton, 1993). The thickness of the weathered regolith, fracture connectivity, lithological variations, recharge conditions, and structural discontinuities largely determine groundwater storage and productivity in crystalline basement terrains.Unlike sedimentary basins, basement aquifers are discontinuous, heterogeneous, and require targeted exploration strategies. The delineation of groundwater potential zones in such terrains remains a significant scientific and practical challenge.

Geophysical methods, particularly electrical resistivity techniques, have proven effective in groundwater exploration due to the strong contrast between saturated weathered/fractured zones and fresh basement rocks (Zohdy *et al*., 1974; Keary and Brooks, 1996). Electrical resistivity surveying has become one of the most widely adopted geophysical techniques because it is relatively inexpensive, non-invasive, rapid, and capable of providing reliable subsurface information for groundwater exploration. Vertical electrical sounding provides quantitative estimates of layer resistivities and thicknesses, from which hydrogeological parameters such as transverse resistance, longitudinal conductance, and transmissivity can be derived (Maillet, 1947; Henriet, 1979; Utom *et al*., 2012). Furthermore, the integration of VES-derived Dar Zarrouk parameters with geographic information system-based multi-criteria decision analysis (e.g., analytical hierarchy process, AHP) enables spatially explicit mapping of groundwater potential (Mogaji *et al*., 2021; Arulbalaji *et al*., 2019).

Recent studies have demonstrated the effectiveness of integrating geophysical techniques with GIS-based multi-criteria decision analysis for groundwater exploration in crystalline basement terrains. Arulbalaji *et al*. (2019) reported that integrating remote sensing, geophysical data, and AHP significantly improved groundwater potential mapping accuracy in southern India. Mogaji *et al*. (2021) successfully applied hydrogeophysical parameters and GIS techniques to delineate productive aquifer zones in southwestern Nigeria. Similar approaches have also been employed in Ethiopia, Ghana, and other parts of sub-Saharan Africa, highlighting the importance of combining geological, structural, hydrological, and geophysical datasets to reduce uncertainties associated with groundwater exploration.

The study area, Mubi and environs in Adamawa State, northeastern Nigeria, lies within the Hawal Basement Complex. Groundwater is the primary water source for domestic and agricultural use, yet no comprehensive hydrogeophysical assessment has been conducted to map aquifer distribution, protective capacity, or potential zones. Despite the growing application of integrated hydrogeophysical and GIS-based techniques worldwide, comparable investigations remain limited within the Hawal Basement Complex of northeastern Nigeria. Existing studies in Mubi and its environs have largely focused on regional geological descriptions or isolated geophysical investigations without integrating geological mapping, quantitative hydrogeophysical parameter estimation, and

GIS-based multi-criteria decision analysis. Consequently, the spatial distribution of aquifer protective capacity, transmissivity, and groundwater potential remains poorly understood, limiting effective groundwater development and sustainable water resource planning.Previous studies in the region have been limited to general geological descriptions (Obaje, 2009; Opeloye and Dio, 1999) or isolated geophysical surveys (Obiefuna *et al*., 2013; Adegokekayode *et al*., 2015). Unlike previous investigations, this study combines detailed geological field mapping, quantitative interpretation of vertical electrical sounding data, estimation of Dar Zarrouk parameters, hydraulic parameter evaluation, and GIS-based analytical hierarchy process to develop a validated groundwater potential map for Mubi and its environs.

Therefore, this study aims to delineate groundwater potential zones in Mubi and environs through an integrated geological, hydrogeophysical, and GIS-based multi-criteria decision analysis approach.

The findings of this study will provide a scientific basis for groundwater exploration, borehole siting, and sustainable groundwater resource management in Mubi and surrounding communities. The integrated methodological framework developed in this study can also be applied in other crystalline basement terrains with similar geological conditions across northeastern Nigeria and sub-Saharan Africa. Furthermore, the groundwater potential map generated from this study will support policymakers, water resource managers, and development agencies in making informed decisions regarding rural water supply, agricultural development, and climate resilience.

1.1 Geological and Hydrogeological Setting

1.1.1 Location and accessibility

The study area (Fig. 1) forms part of the Hawal Basement Complex within the Nigerian Basement Complex, comprising predominantly Pan-African granitoids, migmatitic gneisses, and associated intrusive rocks.

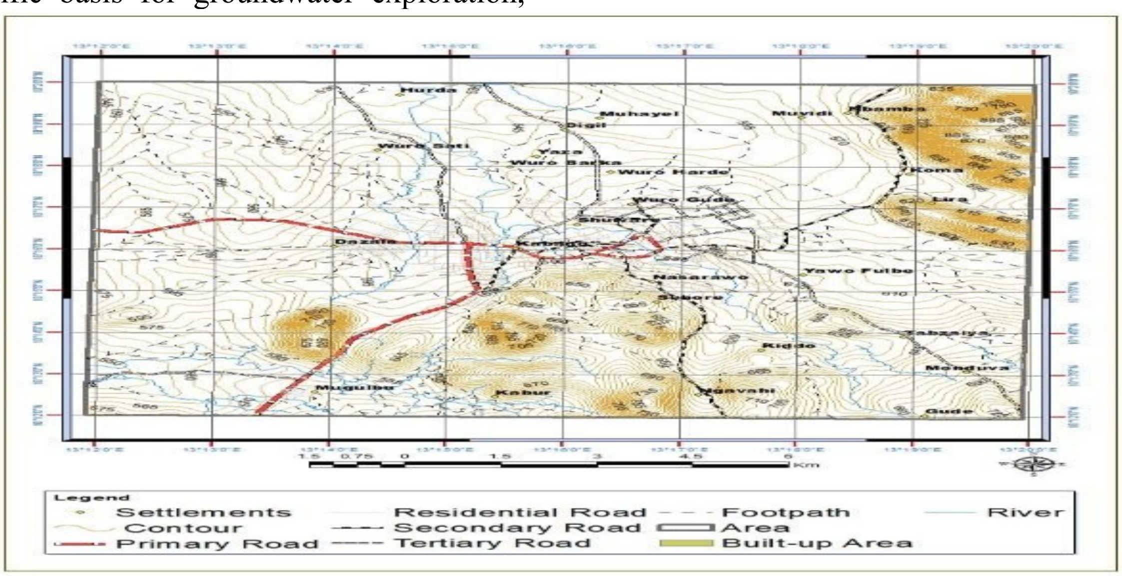

Fig, 1: Location map of the study area showing major settlements, drainage, and road network

In the study area, groundwater occurrence is mainly controlled by weathered overburden, fractured bedrock, and structural discontinuities developed during the Pan-

African tectonic events.The area falls within the basement complex of northeastern Nigeria and covers an area of about 216 km², lying within longitudes 13°12′00″ E to 13°20′00″ E and latitudes 10°12′00″ N to 10°20′00″ N (Fig. 1). Mubi town is located approximately 144 km from Yola and about 25 km from the Nigeria–Cameroon border. The area is readily accessible due to an established road network.

The study area has a tropical climate characterized by distinct dry and wet seasons. The wet season typically commences around April and ends in late October, with average monthly precipitation ranging from 7.5 mm to 330.9 mm. August and September are the wettest months. The dry season extends from late November to early April, coinciding with the Harmattan period, when dust-laden northeasterly trade winds from the Sahara Desert have a marked effect on the climate, making the period cold and dry.

The general relief of the study area is undulating, broken by a network of gullies. The area is characterized by high relief ranging from 775 m above mean sea level in the western part to 855 m above mean sea level in the northern part of the study area.

1.1.2 Geological context

The study area lies within the northern Adamawa State, northeastern Nigeria, located within the Hawal Mountain range—one of the regional groups of basement complex rocks. Obaje (2009) broadly divided the geology of Nigeria into two major geological components: the Basement Complex and the Sedimentary Basins. Oyawoye (1970) further subdivided the basement (Precambrian in age) into five regions based on the occurrence of sedimentary basins: the Western Nigerian Basement, North Central Nigerian Basement, Adamawa Highland, Eastern Nigerian Basement, and the Oban Massif. Except for the older granites, the basement rocks are chiefly migmatitic gneisses, including banded varieties. These rock assemblages, according to Rahaman (1976), are considered the largest component of the Nigerian basement complex.

The Hawal basement is bounded to the north by the Chad Basin (Fig. 2) and to the west and south by the Cretaceous, north-trending Gongola arm and the east-trending Yola arm of the Bamenda Massif of Cameroon, which extends into part of Nigeria (Ekwueme, 1993). The Hawal Massif, a name given to the basement complex of northeastern Nigeria, has seen relatively little work on its geology, stratigraphy, and tectonic events. These basement rocks were emplaced within the Pan-African Mobile Belt of Late Proterozoic (500–750 Ma) age. The rock units are composed dominantly of massive granite plutons in association with diorite and gabbro, collectively termed the older granite, which have been dated elsewhere at 500–750 Ma.

1.1.3 Previous hydrogeological studies

Previous hydrogeological investigations in the Mubi area are limited. Obiefuna *et al*. (1997) provided a preliminary description of the geology and hydrogeology, noting that groundwater occurs in weathered and fractured zones of the basement rocks. Adegokekayode *et al*. (2015) employed remote sensing and GIS techniques to identify groundwater exploration zones, but their study did not include ground-based geophysical validation. The present study therefore represents the first integrated geoelectrical and GIS-based assessment of groundwater potential in this area. However, none of these studies comprehensively integrated geological mapping, hydrogeophysical parameter estimation, aquifer protective capacity assessment, transmissivity analysis, and GIS-based analytical hierarchy process to produce a validated groundwater potential map for Mubi and its environs.

2.0 Materials and Method

2.1 Field geological mapping

Field geological mapping was conducted to establish the lithological distribution and structural framework of the study area. Geological mapping was conducted at a scale of 1:25,000 using a handheld GPS receiver, geological compass-clinometer, and topographic base maps. Lithological boundaries, structural discontinuities, weathering characteristics, and geomorphological features relevant to groundwater occurrence were systematically documented.Five fresh rock samples were collected using a geological field hammer from different locations within the study area. The samples were labeled and submitted for petrographic analysis. Thin sections were prepared and examined under a petrological microscope to identify mineral constituents and textural relationships.

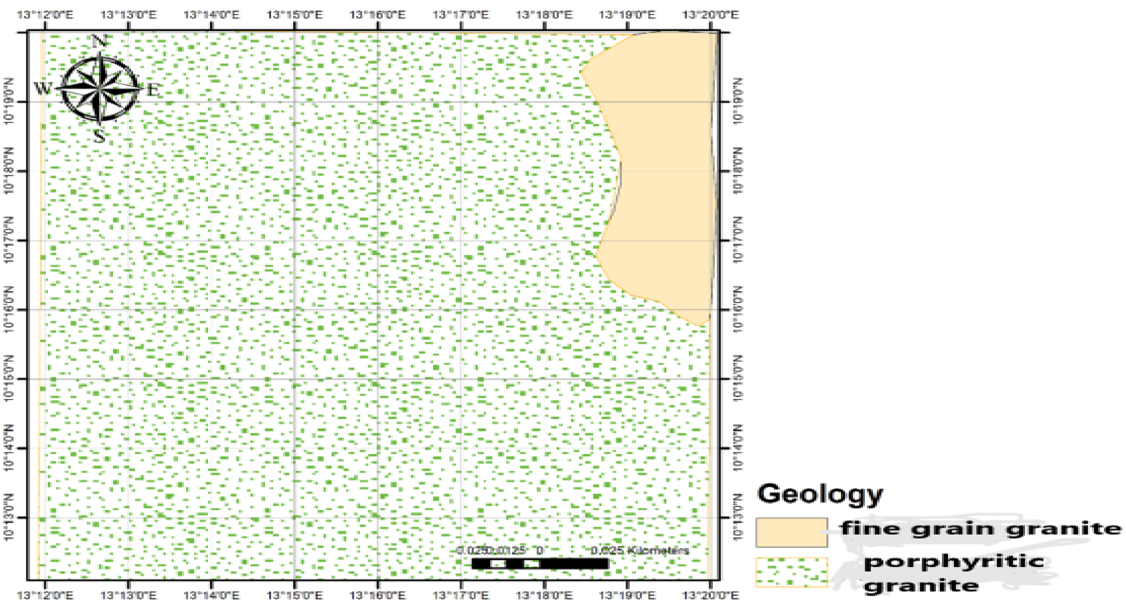

Fig. 2: Geological map of the study area (modified after Geological Survey of Nigeria Agency, 1996)

Structural measurements (joints, faults, and veins) were recorded at outcrop locations. Orientation data were plotted as rose diagrams to identify dominant structural trends.

2.2 Vertical electrical sounding

A total of 40 Vertical Electrical Sounding (VES) stations were surveyed across the study area using a resistivity meter (SAS 6000 Terrameter, ABEM Instrument AB, Sweden). calibrated according to the manufacturer's specifications before commencement of the survey. The Schlumberger electrode configuration was employed, with current electrode spacing (AB/2) ranging from 1 m to 200 m and potential electrode spacing (MN/2) ranging from 0.5 m to 20 m. The maximum spread length was approximately 400 m, providing investigation depths sufficient to penetrate the weathered/fractured zone and reach fresh basement.

VES stations were distributed across the study area to ensure representative coverage of different lithological units and topographic settings. Coordinates of all VES stations were recorded using a handheld global positioning system (GPS). The spacing between adjacent VES stations was selected to provide adequate spatial coverage of the study area while accounting for accessibility, geological variability, and topographic conditions. Measurements were repeated where necessary to minimize observational errors, and noisy data points were re-measured before field completion

2.3 Data processing and interpretation

Apparent resistivity values were initially plotted on bilogarithmic graphs for preliminary curve-type identification before computer-assisted inversion.Qualitative interpretation involved comparing observed field curves with standard master and auxiliary curves (Zohdy *et al*., 1974). Quantitative interpretation was performed using INTERPEX resistivity software (version 4.3, Interpex Limited, USA), which employs an iterative forward modeling and inversion algorithm to generate layered earth models. The interpreted models were validated by comparing calculated apparent resistivity curves with observed field curves.

For each VES station, the inversion process minimized the root-mean-square (RMS) fitting error between measured and calculated apparent resistivity values. Acceptable models were those with RMS errors less than 2.0%. Output parameters included layer resistivities (ρ_1, ρ_2, ρ_3, ρ_4) and layer thicknesses (h_1, h_2, h_3, h_4).

2.4 Dar Zarrouk parameter estimation

Longitudinal conductance (S) and transverse resistance (T) were calculated from the interpreted layer parameters using standard relationships (Maillet, 1947; Henriet, 1979).

Longitudinal conductance (S) is defined as equation 1

$$S = \sum_{i=1}^{n} \frac{h_i}{p_i} \quad (1)$$

where h_i is the thickness of layer i (m), p_i is the resistivity of layer i (Ω·m), and n is the number of layers.

Transverse resistance (T) is defined according to equation 2

$$T = \sum_{i-1}^{n} h_i p_i \quad (2)$$

These parameters were calculated for each VES station up to the depth of the weathered/fractured zone or fresh basement.

2.5 Estimation of hydraulic parameters

Hydraulic conductivity (K) and transmissivity (T_r) were estimated from the electrical resistivity data using empirical relationships established for basement complex terrains. Following the approach of Heigold *et al*. (1979) and Niwas and Singhal (1981), the relationship between aquifer resistivity and hydraulic conductivity is expressed according to equation 3

$$logK = alogp + b \quad (3)$$

where aa nd b are empirically derived constants. For this study, the relationship established for crystalline basement terrains in Nigeria (Oladapo and Akintorinwa, 2007) was adopted.

Transmissivity (T_r, $m^2 \cdot d^{-1}$) was calculated using equation 4

$$T_r = k \times h \quad (4)$$

where K is hydraulic conductivity ($m \cdot d^{-1}$) and h is the saturated thickness of the aquifer (m), taken as the thickness of the weathered/fractured zone. Hydraulic conductivity values estimated from resistivity data represent indirect approximations and are appropriate for regional groundwater potential assessment rather than detailed aquifer performance evaluation.

2.6 GIS-based analytical hierarchy process

A GIS-based multi-criteria decision analysis was implemented using the analytical hierarchy process (Saaty, 1980). Seven thematic layers were prepared:

1. Geology – derived from field mapping
2. Land use/land cover – derived from Landsat 8 OLI imagery
3. Soil type – derived from soil survey data (Soil Survey Staff, 1975)
4. Rainfall – interpolated from 10-year rainfall records (2005–2015)
5. Lineament density – extracted from digitally enhanced satellite imagery

6. Drainage density – computed from drainage network extracted from a digital elevation model (ASTER GDEM)
7. Slope – computed from the same digital elevation model

Each thematic layer was classified and assigned a weight based on pairwise comparison following Saaty's (1980) fundamental scale of 1 to 9. The consistency ratio was calculated to verify the reliability of the pairwise comparison matrix. A consistency ratio ≤ 0.10 was considered acceptable.

Weighted overlay analysis was performed in ArcGIS 10.5 (ESRI, Redlands, CA, USA) to produce the final groundwater potential map.

3.0 Results and Discussion

3.1 Results

3.1.1. Lithological units and petrography

The lithological units identified within the study area consist predominantly of porphyritic granite (Fig. 3a) and fine-grained granite (Fig. 3b). In several parts of the area, these basement rocks are overlain by eluvial deposits derived from the in-situ weathering of the underlying crystalline rocks. The eluvial materials are mainly distributed within the southwestern and southeastern portions of the study area. The distribution of these weathered materials is hydrogeologically significant because they constitute the principal regolith aquifer in crystalline basement terrains. Areas with thicker weathered overburden generally possess higher groundwater storage capacity due to enhanced porosity and permeability.

Structural geology

The eluvial deposits can be classified into two categories: recent river-course alluvium and older eluvial deposits. The recent river-course alluvium is confined to the floodplains of the River Yedsarem and some of its tributaries and is composed mainly of fine- to medium-grained sands and clayey materials.

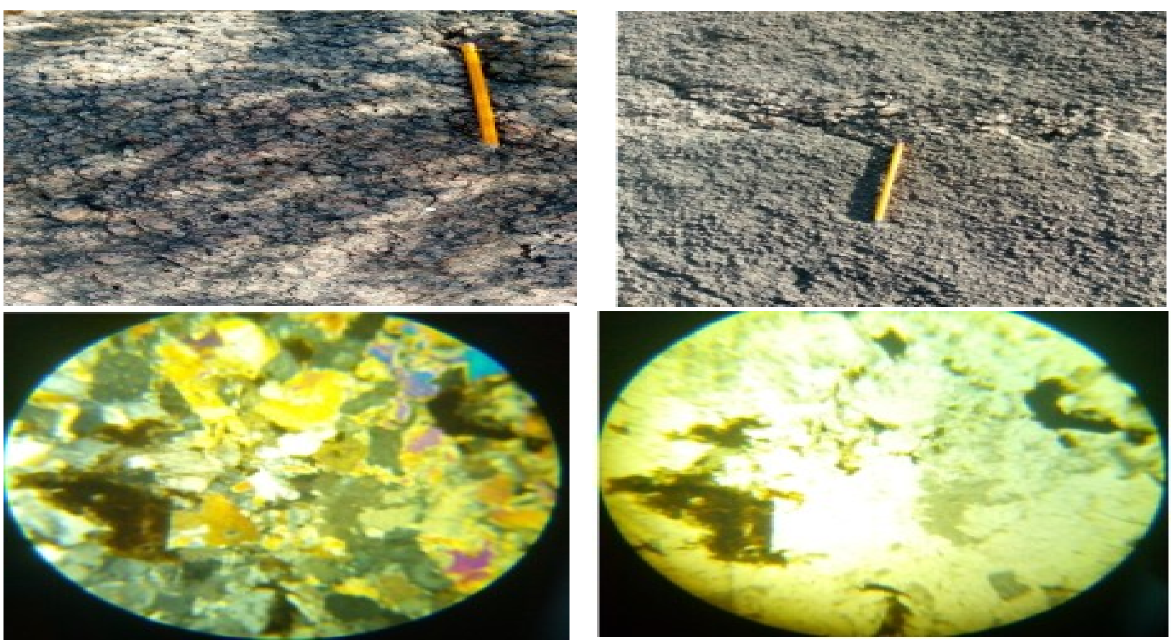

Figs. 3. (a) Field photograph of porphyritic granite at Madanya-Mubi showing large feldspar phenocrysts (top left) (b) Field photograph of fine-grained granite at Koma-Lira Mubi. (c) Photomicrograph of porphyritic granite under cross-polarized light (×40 magnification). (d) Photomicrograph of porphyritic granite under plane-polarized light (×40 magnification). All photomicrographs include a 500 µm scale bar (bottom right)

In some locations, particularly around Mararaba Mubi, the basement rocks are overlain by reddish-brown lateritic materials, believed to have formed through in-situ weathering processes.

Areas such as Lira and Vintim are underlain predominantly by fine-grained granitic rocks characterized by alternating light- and dark-colored mineral bands. The observed variations in mineral composition and texture may influence the intensity of weathering, fracture development, and consequently groundwater productivity.Petrographic analysis of thin sections revealed that the light-colored bands are composed mainly of quartz and microcline feldspar, whereas the dark-colored bands consist predominantly of biotite and hornblende (Figs. 3c and3d).

According to Oyawoye (1970), such banding is associated with the emplacement of pegmatite dykes and quartz-feldspar veins along foliation planes within migmatitic rocks, suggesting that the parent rocks were originally gneissic and subsequently underwent partial melting and metamorphism to form migmatites.

Granitic rocks dominate areas such as Sahuda, where they occur as coarse-grained bodies exhibiting both granular and porphyritic textures. These textural characteristics indicate a slow cooling history and crystallization at considerable depths within the crust.

The granitic rocks within the study area are predominantly potassic granites, which grade into relatively more mafic varieties toward the margins of the intrusions. Both the composition and texture of the porphyritic granites exhibit noticeable variations from the centre of the intrusion toward its margins. At the central portions of the intrusions, feldspar phenocrysts are densely packed, giving the rock a relatively homogeneous biotite granite appearance. Toward the margins, the abundance of feldspar phenocrysts gradually decreases, resulting in a less porphyritic texture.

The major structural features identified within the study area include joints, fractures, faults, folds, and veins (Fig. 4a). Among these, quartz veins (Fig. 4b) are the most abundant and occur predominantly within outcrop exposures in the northern part of the study area, although minor pegmatite veins were also observed.

Field measurements of joint and fault orientations, together with lineament data extracted from remote sensing analyses, were used to generate rose diagrams (Figs. 5a, 5b). The resulting plots reveal a pronounced preferential orientation in the NE–SW direction across the study area. The fracture rose diagram exhibits a bidirectional pattern, with the dominant structural trend occurring in the NE–SW direction. This trend corresponds closely with the regional structural fabric established during the Pan-African Orogeny, which imposed a dominant N–S to NNE–SSW structural orientation on the Nigerian Basement Complex (Russ, 1957; McCurry, 1973; Rahaman, 1976; Obaje, 2009).

Similarly, the lineament rose diagram (Fig. 5b) indicates dominant orientations in the NNE–SSW direction, further reflecting the influence of Pan-African tectonism on the structural framework of the area. According to Odeyemi *et al*. (1999), NE–SW-trending lineaments are among the longest and most persistent structural features within the Nigerian Basement Complex and are commonly interpreted as deep-seated crustal structures.

3.1.2 Resistivity data and curve types

Quantitative interpretation of the 40 VES stations produced layer parameters for each sounding. A representative summary of the interpreted data is presented in Table 1. The complete VES dataset is provided as Supplementary Material (Table S1).

Fig. 4: (a) Normal fault displacing fine- to coarse-grained granite at Nzire. Hammer for scale (35 cm). (b) Quartz vein intruding porphyritic granite at Madanya. Scale card (10 cm) for reference.

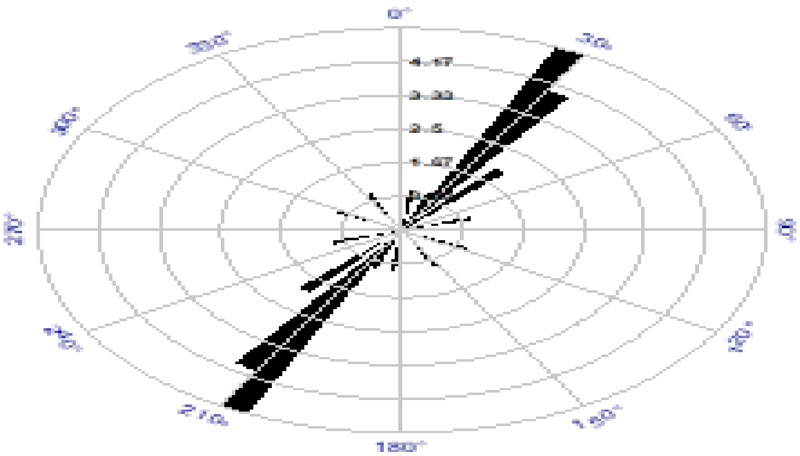

Fig, 5. Lineanment rose diagram

Table 1: Summary of interpreted VES parameters for 40 stations

Parameter	Minimum	Maximum	Mean	Standard Deviation
Layer 1 thickness (m)	0.16	25.88	1.89	4.03
Layer 2 thickness (m)	0.45	39.66	11.81	9.87
Layer 3 thickness (m)	2.14	76.39	21.75	18.56
Layer 1 resistivity (Ω·m)	9.43	3086.30	168.17	477.62
Layer 2 resistivity (Ω·m)	7.55	439.21	48.58	65.18
Layer 3 resistivity (Ω·m)	7.75	2168.00	262.56	425.51
Layer 4 resistivity (Ω·m)	59.05	3897.10	639.12	981.63
RMS fitting error (%)	0.43	0.99	0.86	0.12

The analyzed sounding curves obtained from the different locations show that 62.5% of the curves are dominated by the H-type curve, 15% are the KH curve type, 12.5% are the QH curve, and 10% are the A-type curve (Fig, 6). The H-type curve, characterized by a central low-resistivity layer sandwiched between higher-resistivity layers, typically indicates a weathered/fractured zone overlying fresh basement.

The predominance of H-type curves indicates that weathered basement aquifers constitute the principal groundwater-bearing horizon within the study area. This curve type is widely regarded as favorable for groundwater development because the intermediate low-resistivity layer commonly represents saturated weathered materials overlying competent basement.

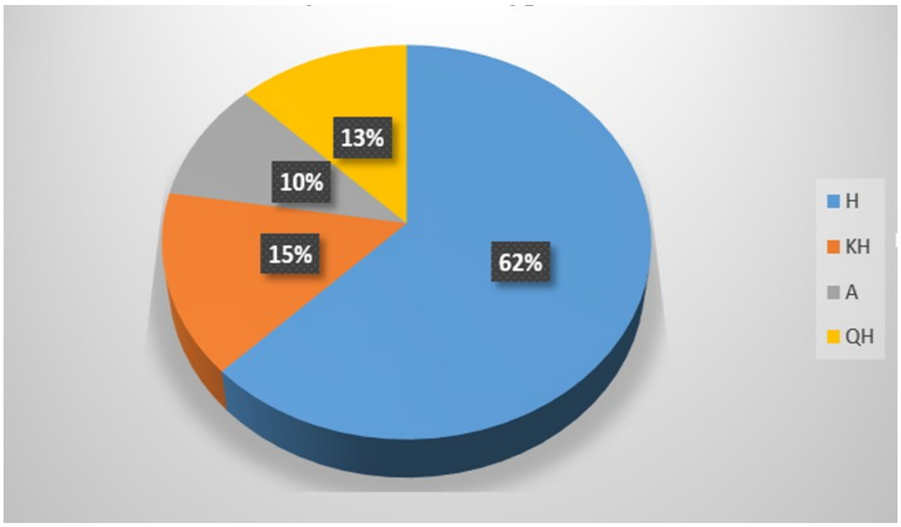

Fig, 6. Distribution of VES curve types in the study area (n = 40). H-type curves constitute 62.5%, KH 15%, QH 12.5%, and A-type 10%.

3.1.3 Dar Zarrouk parameters

The longitudinal conductance (S) in the study area ranges from 0.01 Ω^{-1} (VES 33) to 4.51 Ω^{-1} (VES 27), with a mean value of 0.69 Ω^{-1} (Table 1). The transverse resistance (T) ranges from 12.38 $\Omega\cdot m^2$ (VES 15) to 5029.51 $\Omega\cdot m^2$ (VES 28), with a mean value of 1347.03 $\Omega\cdot m^2$.

3.1.4 Hydraulic conductivity and transmissivity

Hydraulic conductivity values estimated from the resistivity data range from 1.32 $m\cdot d^{-1}$ to 58.62 $m\cdot d^{-1}$. Transmissivity values range from 5.89 $m^2\cdot d^{-1}$ to 748.78 $m^2\cdot d^{-1}$, with a mean value of 333.01 $m^2\cdot d^{-1}$. These values indicate moderate to high groundwater transmission capacity and are consistent with productive weathered and fractured basement aquifers reported elsewhere in the Nigerian Basement Complex.

3.2 Discussion

3.2.1 Geoelectric sections and aquifer delineation

Correlation of the geo-electric sections obtained from VES interpretation with borehole lithologic logs was carried out to establish the relationship between electrical properties and subsurface geological formations. Three correlation profiles, designated A–A′, B–B′, and C–C′, were constructed across the study area (Fig, 7).

Profile A–A′ (Fig, 8) trends in a southeast–northwest direction and passes through Borehole 1 (BH1), VES 25, VES 30, and VES 7. The correlation reveals that the first geo-electric layer corresponds to the topsoil and is present throughout the profile, with thicknesses ranging from 0.63 m to 18.40 m. The second layer is predominantly a weathered basement unit, with thicknesses ranging from 2.07 m to 25.26 m. The third layer consists of fresh basement rock in VES 30, VES 7, and BH1, but at VES 25, the third layer is interpreted as a fractured basement with a thickness of 17.47 m, underlain by fresh basement. The principal aquifer units within this profile are the weathered and fractured basement zones.

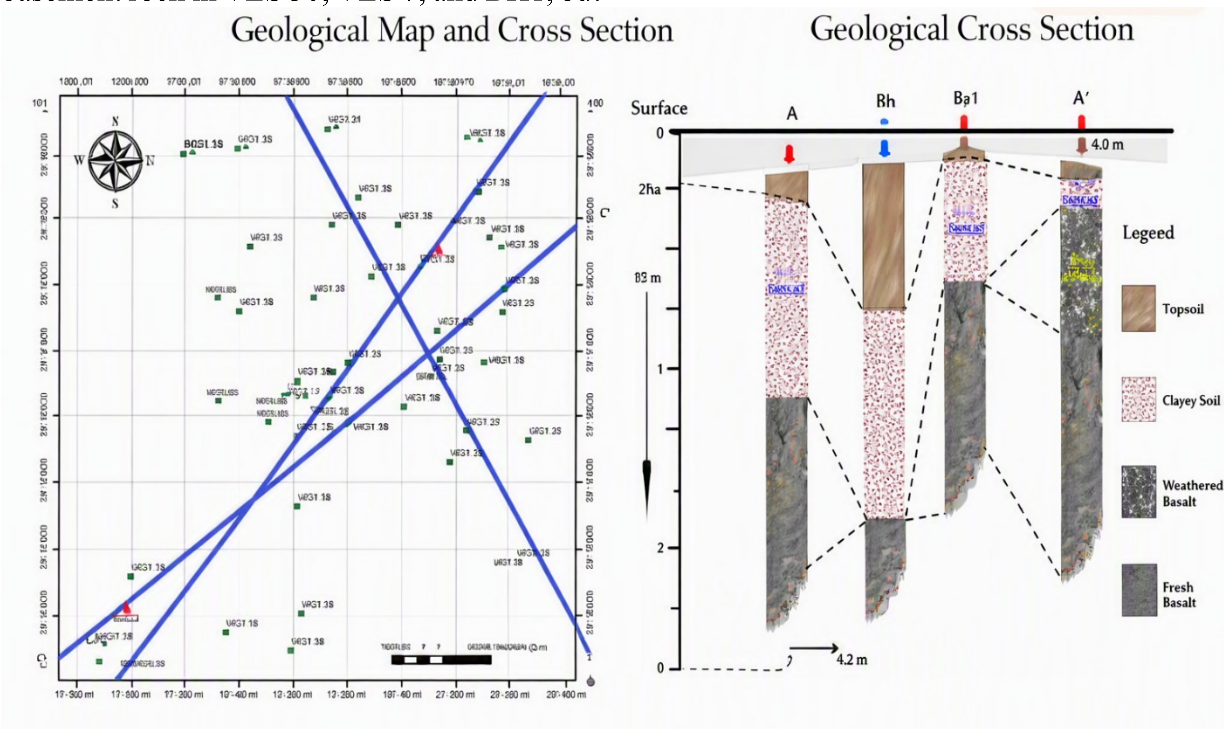

Fig. 7. Map showing the location of VES stations, boreholes, and correlation profiles (A–A′, B–B′, C–C′) used for geo-electric section construction. Fig. 8. Correlation of geo-electric and lithologic sections along profile A–A′ showing weathered and fractured basement as the principal aquifer units.

Profile B–B′ (Fig, 9) trends in a southwest–northeast direction and comprises VES 11, VES 2, VES 22, and Borehole 2. The first layer (topsoil) thickness varies from 0.73 m to 9.20 m. The second layer is a highly weathered basement unit (thickness 6.96–17.08 m) in VES 11 and VES 22, but at VES 2 it is thinner (0.67 m). In Borehole 2, the corresponding layer consists of brown clay (thickness ~23.00 m), which likely exhibits similar resistivity characteristics to weathered basement. The third layer at VES 2 is a weathered/fractured basement (19.10 m), indicating enhanced groundwater potential.

Profile C–C′ (Fig, 10) comprises Borehole 3, VES 12, and VES 9. The first layer (topsoil/thickness 0.82–4.20 m) is underlain by a weathered basement (thickness 7.22–23.40 m). The third layer is identified as a fractured basement in VES 12 and BH3 (thicknesses 23.78 m and 27.60 m, respectively), representing zones of enhanced secondary porosity. At VES 9, the third layer is fresh basement.

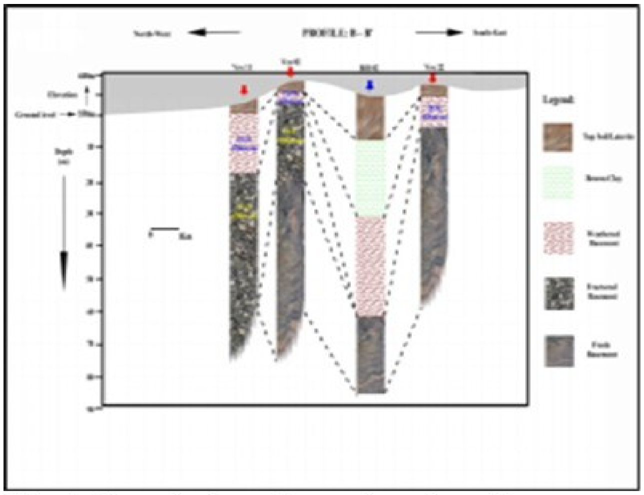

Fig. 9:Correlation of geo-electric and lithologic sections along profile B–B′

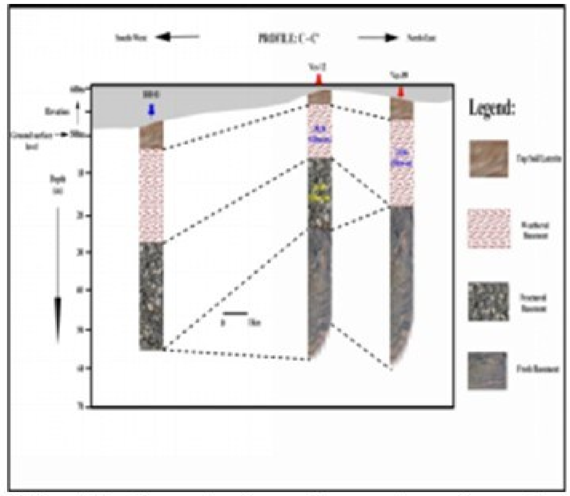

Fig. 10: Correlation of geo-electric and lithologic sections along profile C–C′

The correlation demonstrates that the principal aquifer units in the study area are the weathered and fractured basement zones. These units possess enhanced porosity and permeability resulting from weathering and structural deformation, making them favorable groundwater reservoirs in basement complex terrain.

3.2.2 Aquifer protective capacity

The aquifer protective capacity was evaluated using longitudinal conductance values, following the classification of Oladapo and Akintorinwa (2007) (Table 2).

Approximately 82.5% of the VES stations exhibit moderate to good protective capacity, indicating that most aquifers possess appreciable natural attenuation potential against surface-derived contaminants.

The moderate protective capacity class is the most extensive, covering approximately 47.5% of the study area, particularly around Kabur, Lamurde, Shuwari, and Gidan Madara. Areas with good protective capacity are predominantly located in the northern and southern parts, including Koma, Lira, Hurida, Monduva, and Mugulbu. The weak to poor protective capacity zones occur as isolated patches around Kekeba, Dazala, Digil Village, and GDSS Vintim, where aquifers are more susceptible to contamination.

Table 2: Classification of aquifer protective capacity (after Oladapo and Akintorinwa, 2007)

Longitudinal conductance (Ω^{-1})	Protective capacity
> 10	Excellent
5 – 10	Very good
0.7 – 4.9	Good
0.2 – 0.69	Moderate
0.1 – 0.19	Weak
< 0.1	Poor

The predominance of moderate to good protective capacity classes suggests that the study area possesses generally favorable aquifer protection characteristics, although localized zones of weak and poor protective capacity require careful groundwater management.

Analysis of the results (Table 3; Fig, 11) shows that 14 VES stations (35%) possess good protective capacity, 19 VES stations (47.5%) fall within the moderate protective capacity category, 5 VES stations (12.5%) exhibit weak protective capacity, and 2 VES stations (5%) have poor protective capacity.

Table 3 : Summary of aquifer protective capacity classification

Protective capacity	Number of VES stations	Percentage (%)
Good	14	35.0
Moderate	19	47.5
Weak	5	12.5
Poor	2	5.0
Total	40	100

3.2.3 Groundwater potential from transmissivity

Transmissivity values were used to classify aquifer potential following the scheme of Offodile (1983) and Ezeh (2002) (Table 4). The results indicate that 31 VES stations (77.5%) have moderate potential, 7 VES stations (17.5%) have high potential, and 2 VES stations (5%) have low potential (Table 4; Fig, 12).

Table 4: Classification of aquifer potential based on transmissivity.

Transmissivity ($m^2 \cdot d^{-1}$)	Aquifer potential	Number of VES stations	Percentage (%)
> 500	High	7	17.5
50 – 500	Moderate	31	77.5
< 50	Low	2	5.0

The spatial distribution of transmissivity (Fig, 12) reveals that areas with high transmissivity (designated by brown to red colours) are concentrated in the central part of the study area, particularly around VES 27 (Harde). Moderate transmissivity values (green colours) cover approximately 70% of the study area, extending across the northern, southwestern, and southeastern portions. Low transmissivity values (dark blue to light blue colours) occur in the northwestern, northeastern, and south-south parts of the map.

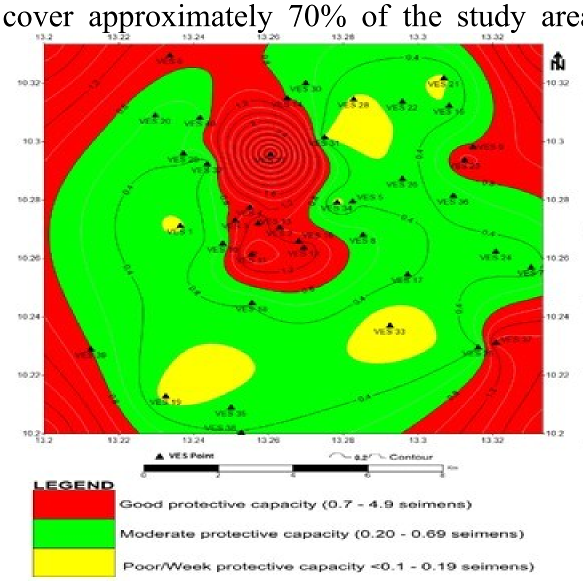

Fig. 11: Spatial distribution map of aquifer protective capacity based on longitudinal conductance values

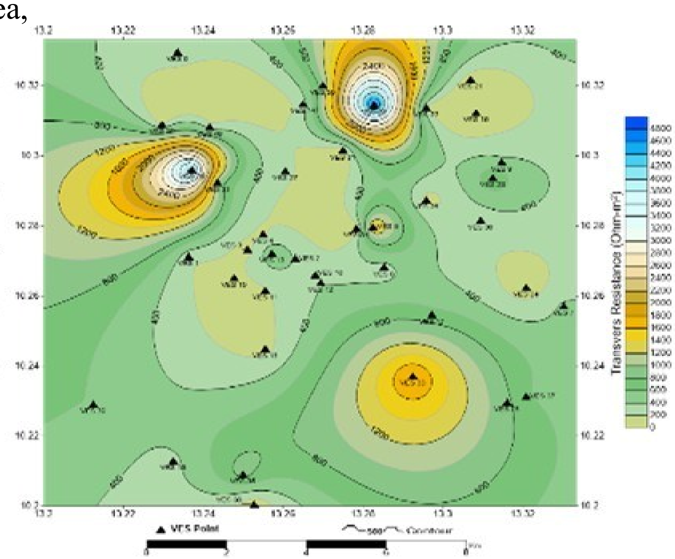

Fig. 12: Spatial distribution map of transmissivity in the study area

3.2.4 GIS-based analytical hierarchy process

The analytical hierarchy process produced a groundwater potential map classifying the study area into three zones: poor, moderate, and good potential (Fig. 13).These zones correspond closely with areas exhibiting high lineament density, moderate slopes, thicker weathered overburden, and elevated transmissivity, demonstrating the effectiveness of integrating hydrogeophysical parameters with GIS-based multi-criteria analysis. The consistency ratio for the pairwise comparison matrix was calculated as 0.0049, which is well below the acceptable threshold of 0.10 (Saaty, 1980), confirming the reliability of the weighting.

The groundwater potential index values indicate that areas with high potential are concentrated in the southern part of the study area, particularly around VES 18, 19, 25, 35, 37, 38, and 39, as well as at the boundaries of the study area. These areas are characterized by a combination of favorable factors: low to average slope, high lineament density, appropriate land use/cover, and suitable geological conditions.

3.2.5 Comparison with regional studies

The predominance of H-type curves (62.5%) in the study area is consistent with findings from other basement complex terrains in Nigeria. Abiola *et al*. (2009) reported a similar dominance of H and HK curves in Ado-Ekiti, southwestern Nigeria. Utom *et al*. (2012) found that H-type curves constitute approximately 58% of VES soundings in parts of Enugu Town. The mean transverse resistance (1347 Ω·m²) obtained in this study is comparable to values reported from the Ogun drainage basin (Aladeboyeje *et al*., 2021) but significantly higher than those from coastal Lagos (Fatoba *et al*., 2014), reflecting the thicker weathering profiles typical of the humid tropical climate of northeastern Nigeria.

The NE–SW dominant structural trend observed in both fracture and lineament rose diagrams corroborates the regional Pan-African structural grain documented by Russ (1957), McCurry (1973, 1976), and Rahaman (1976). This trend suggests that regional tectonic fabrics exert primary control on groundwater occurrence in the Hawal Basement Complex, as fractures and joints oriented along this direction provide the most favorable pathways for groundwater circulation.

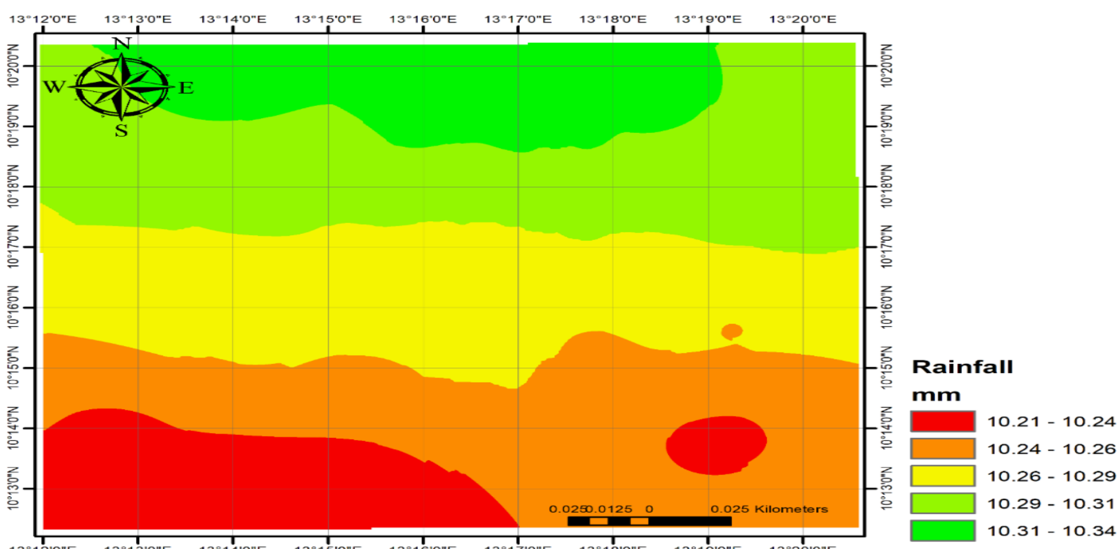

Fig. 13: Groundwater potential map produced from GIS-based Analytical Hierarchy Process showing poor, moderate, and good potential zones

The transmissivity values (mean 333 $m^2 \cdot d^{-1}$) are within the range reported for weathered/fractured basement aquifers in Nigeria. Offodile (1983) reported transmissivity values ranging from 5 to 800 $m^2 \cdot d^{-1}$ for basement aquifers across Nigeria, while Mogaji *et al*. (2021) reported mean transmissivity of 284 $m^2 \cdot d^{-1}$ for a similar terrain in southwestern Nigeria.

2.2.6 Limitations and uncertainties

Several limitations of this study should be acknowledged. First, the estimation of hydraulic conductivity and transmissivity from resistivity data relies on empirical relationships that may introduce uncertainty. Direct pumping tests, while expensive, would provide more accurate aquifer parameters. Second, the VES method assumes horizontal layering, which may not fully capture the complex, heterogeneous nature of fractured basement aquifers. Third, the AHP weighting, although consistent, involves subjective judgments in the pairwise comparison process. Future studies should incorporate borehole yield data to validate the groundwater potential map.

4.0 Conclusion

This study successfully delineated groundwater potential zones in Mubi and environs, northeastern Nigeria, using an integrated approach combining geological field mapping, vertical electrical sounding, Dar Zarrouk parameters, transmissivity estimation, and GIS-based analytical hierarchy process. The following conclusions are drawn:

1. The study area is underlain predominantly by porphyritic granite and fine-grained granite of the Pan-African basement complex. Major structural features include joints, faults, and veins with a dominant NE–SW orientation that reflects regional Pan-African tectonism.
2. Analysis of 40 VES stations revealed four curve types: H (62%), KH (15%), A (10%), and QH (13%), indicating weathered and fractured/weathered aquifer systems. Three to four geo-electric layers were delineated: topsoil, weathered basement, fractured/weathered basement, and fresh basement.
3. Aquifer protective capacity, assessed using longitudinal conductance (0.01–4.51 Ω^{-1}), is moderate (47.5% of the area) to good (35%), suggesting generally favorable natural attenuation of surface contaminants. Weak to poor protective capacity occurs in localized patches (17.5% combined).
4. Transmissivity values (5.89–748.78 $m^2 \cdot d^{-1}$; mean 333.01 $m^2 \cdot d^{-1}$) classify the aquifer potential as moderate (77.5%) to high (17.5%), with only 5% low potential.
5. The GIS-based AHP produced a groundwater potential map with a consistency ratio of 0.0049, confirming reliable weighting. High potential zones are concentrated in the southern part of the study area, particularly around VES 18, 19, 25, 35, 37, 38, and 39.
6. The integrated geoelectrical and GIS approach demonstrated here is replicable for groundwater targeting in analogous crystalline basement terrains across sub-Saharan Africa, providing a cost-effective framework for water resource evaluation in data-scarce regions.

For sustainable groundwater development in Mubi and environs, it is recommended that borehole drilling prioritize areas with good protective capacity and high transmissivity. Localized zones of weak to poor protective capacity should be avoided for groundwater abstraction or subjected to regular water quality monitoring.

Acknowledgements

I want to express my sincere appreciation to Modibbo Adama University Yola, Adamawa State and the individuals whose contributions and support have greatly enhanced the quality of this research. I am grateful to my primary supervisor Prof. J. M Ishaku for his unwavering guidance, insightful suggestions and constant encouragement. I am grateful to National Center for Remote Sensing, Jos Plateau State.

5.0 References

Abiola, O., Enikanselu, P. A., & Oladapo, M. I. (2009). Groundwater potential and aquifer protective capacity of overburden units in Ado-Ekiti, southwestern Nigeria. *International Journal of Physical Sciences*, 4, pp. 120–132.

Adegokekayode, M., Raji, M., & Olayinka, B. B. (2015). Groundwater exploration zones of Mubi Local Government of Adamawa State using remote sensing and geographical information system. *International Journal of Geology and Earth Sciences*, 1, pp. 40–49.

Aladeboyeje, A. I., Coker, J., Agbasi, O. E., & Inyang, N. J. (2021). Integrated hydrogeophysical assessment of groundwater potential in the Ogun drainage basin, Nigeria. *International Journal of Energy and Water Resources*, 5, pp. 36–44.

Arulbalaji, P., Padmalal, D., & Sreelash, K. (2019). GIS and AHP techniques based delineation of groundwater potential zones: A case study from Southern Western Ghats, India. *Scientific Reports*, 9, pp. 2082.

Das, S., Gupta, A., & Ghosh, S. (2017). Exploring groundwater potential zones using MIF technique in semi-arid region: A case study of Hingoli district, Maharashtra. *Spatial Information Research*, 25, pp. 749–756.

Ekwueme, B. N. (1993). Preliminary zircon evaporation ages from migmatite gneiss in Kaduna, northern Nigeria: Evidence for an Archean event in the Nigerian Basement Complex. *Journal of Mining and Geology*, 29, pp. 1–8.

Ezeh, C. C. (2002). Hydrogeophysical studies for the delineation of potential groundwater zones in Enugu State, Nigeria. *International Research Journal of Geology and Mining*, 2, pp. 103–112.

Fatoba, J. O., Omolayo, S. D., & Adigun, E. O. (2014). Using geoelectric soundings for estimation of hydraulic characteristics of aquifers in the coastal area of Lagos, southwestern Nigeria. *International Letters of Natural Sciences*, 11, pp. 30–39.

Foster, S. S. D., & Chilton, P. J. (1993). Groundwater: The world's hidden asset. In *Proceedings of the International Conference on Groundwater Quality*. Nairobi, Kenya.

Heigold, P. C., Gilkeson, R. H., Cartwright, K., & Reed, P. C. (1979). Aquifer transmissivity from surficial electrical methods. *Ground Water*, 17, pp. 338–345.

Henriet, J. P. (1979). Direct applications of the Dar Zarrouk parameters in ground water surveys. *Geophysical Prospecting*, 24, pp. 345–353.

Keary, P., & Brooks, M. (1996). *An introduction to geophysical exploration* (2nd ed.). Blackwell Scientific Publications.

Maillet, R. (1947). The fundamental equations of electrical prospecting. *Geophysics*, 12, pp. 529–556.

Manap, M. A., Nampak, H., Pradhan, B., Lee, S., Sulaiman, W. N. A., & Ramli, M. F. (2011). Application of probabilistic-based frequency ratio model in groundwater potential mapping using remote sensing data and GIS. *Arabian Journal of Geosciences*, 7, pp. 711–724.

McCurry, P. (1973). *Geology of degree sheet 21, Zaria, Nigeria*. Overseas Geology and Mineral Resources, 45, pp. 1–30.

McCurry, P. (1976). The geology of the Precambrian to Lower Palaeozoic rocks of northern Nigeria: A review. In C. A. Kogbe (Ed.), *Geology of Nigeria* (pp. 15–39). Elizabethan Publishing Company.

Mogaji, K. A., Ezekiel, G. I., & Abodunde, O. O. (2021). Modeling of aquifer potentiality using GIS-based knowledge-driven technique: A case study of hard rock geological setting, southwestern Nigeria. *Sustainable Water Resources Management*, 7, pp. 64.

National Water Policy. (1987). *Federal Republic of Nigeria*. Government Printer.

Niwas, S., & Singhal, D. C. (1981). Estimation of aquifer transmissivity from Dar-Zarrouk parameters in porous media. *Journal of Hydrology*, 50, pp. 393–399.

Obaje, N. G. (2009). *Geology and mineral resources of Nigeria*. Springer.

Obiefuna, G. I., Adamolekun, S. S., & Ishaku, J. M. (2013). Determining potential areas of groundwater occurrences using remote sensing techniques: A case study of Mubi area, northeast Nigeria. *Continental Journal of Applied Sciences*, 5, pp. 15–24.

Obiefuna, G. I., Bassey, N. E., Ezeigbo, H. I., & Dahu, N. S. (1997). The geology and hydrogeology of Mubi and its environs, northeast Nigeria. *Water Resources – Journal of National Association of Hydrogeologists*, 8, pp. 41–44.

Obiefuna, G. I., Bassey, N. E., Ezeigbo, H. I., & Dahu, N. S. (1997). The geology and hydrogeology of Mubi and its environs, northeast Nigeria. *Water Resources – Journal of National Association of Hydrogeologists*, 8, pp. 41–44.

Odeyemi, I. B., Anifowose, A. Y. B., & Asiwaju-Bello, Y. A. (1999). Remote sensing fracture characteristics of Pan-African granite batholiths in the basement complex of parts of southwestern Nigeria. *Journal of Technoscience*, 3, pp. 56–60.

Offodile, M. E. (1983). The occurrence and exploitation of groundwater in the Basement Complex of Nigeria. *Journal of Mining and Geology*, 20, pp. 131–146.

Oladapo, M. I., & Akintorinwa, O. J. (2007). Hydrogeophysical study of Ogbese, southwestern Nigeria. *Global Journal of Pure and Applied Sciences*, 13, pp. 55–61.

Opeloye, S. A., & Dio, C. J. (1999). Geology and mineral resources of Adamawa State. In A. A. Adebayo & A. I. Tukur (Eds.), *Adamawa State in Maps*. Paraclete Publishers.

Oyawoye, M. O. (1970). The geology of some northern Nigeria ring complexes. *Geology and Mineralogy*, 6, pp. 421–434.

Rahaman, M. A. (1976). Review of the basement geology of southwestern Nigeria. In C. A. Kogbe (Ed.), *Geology of Nigeria* (pp. 41–58). Elizabethan Publishing Company.

Rahaman, M. A. (1988). Recent advances in the study of the basement complex of Nigeria. In P. O. Oluyide (Coordinator), *Precambrian Geology of Nigeria* (pp. 11–43). Geological Survey of Nigeria.

Russ, W. (1957). The geology of parts of Niger, Zaria, and Sokoto provinces. *Geological Survey of Nigeria Bulletin*, 27, pp. 1–42.

Saaty, T. L. (1980). *The analytical hierarchy process: Planning, priority setting, resource allocation*. McGraw-Hill.

Soil Survey Staff. (1975). *Soil taxonomy: A basic system of soil classification for making and interpreting soil surveys*. USDA Soil Conservation Service.

Taylor, R. G., Scanlon, B., Döll, P., Rodell, M., van Beek, R., Wada, Y., et al. (2013). Ground water and climate change. *Nature Climate Change*, 3, pp. 322–329.

Utom, A. U., Odoh, B. I., & Okoro, A. U. (2012). Estimation of aquifer transmissivity using Dar Zarrouk parameters derived from surface resistivity measurements: A case history from parts of Enugu Town, Nigeria. *Journal of Water Resource and Protection*, 4, pp. 993–1000.

Zohdy, A. A. R., Eaton, G. P., & Mabey, D. R. (1974). *Application of surface geophysics to ground-water investigations*. Techniques of Water-Resources Investigations, United States Geological Survey.

Declarations

Funding

The authors received no financial support for the research, authorship, and/or publication of this article.

Ethical Approval

Not applicable

Informed Consent

Not applicable.

Consent for Publication

Not applicable.

Declaration of Competing Interests

The authors declared no competing financial interests or personal relationships that could have influenced the work reported in this paper.

Data Availability Statement

The datasets generated and/or analyzed during the current study are available from the corresponding author upon reasonable request.

Conflict of Interest

The authors declare that there is no conflict of interest regarding the publication of this manuscript.

Author Contributions

David John Zirra conceived and designed the study, conducted field investigations, analyzed and interpreted geophysical and GIS data, and prepared the manuscript. Umar Ibrahim Ashaka contributed to data interpretation, manuscript review, editing, validation of results, and overall supervision of the research work.

Publisher's Note

The authors are solely responsible for the content and conclusions presented in this study.